Ocean Engineering 105 (2015) 206–216

Contents lists available at ScienceDirect

Ocean Engineering

journal homepage: www.elsevier.com/locate/oceaneng

Thrust allocation algorithm with efficiency function dependent on the azimuth angle of the actuators

F. Arditti, F.L. Souza, T.C. Martins, E.A. Tannuri *

University of São Paulo, Mechatronics Engineering Department, Av. Prof. Luciano Gualberto, travessa 3 no. 380, CEP, São Paulo, 05508-010 SP, Brazil

ARTICLE INFO

Article history:
Received 29 April 2014
Accepted 15 June 2015
Available online 10 July 2015

Keywords:
Thrust allocation
Algorithm
Hydrodynamic interactions
Efficiency
Simulation

ABSTRACT

The Dynamic Positioning System is responsible for the station keeping of the vessel in a variety of offshore operations. The thrust allocation algorithm distributes the required forces among the available thrusters of the vessel accurately whilst optimizing the power consumption. Recent experimental studies and Computational Fluid Dynamics (CFD) simulations have shown that hydrodynamic interaction effects affect the thrust generation. Therefore, the allocation algorithm can be improved if these interactions are considered, using the thrusters efficiency functions in the formulation of the optimization problem. The result of this implementation is a nonlinear optimization problem, solved by a modified Sequential Quadratic Programming technique. The numerical simulations and experimental tests demonstrated a power reduction between 2% and 5% when the proposed thrust allocation algorithm is compared with a forbidden zone allocation (does not allow positioning the thrusters in directions with severe hydrodynamic interactions). The experimental results highlight the advantages of taking the hydrodynamic interactions into account in the thrust allocation algorithm.

1. Introduction

1.1. Dynamic Positioning (DP) System

The DP System is an alternative to the conventional mooring system, in situations in which it is neither possible nor economically feasible to moor the vessel. The DP System is responsible for the station keeping of the vessel, thus allowing it to perform offshore operations, e.g. drilling, offloading, and pipe-laying.

Briefly, the DP System is a *Control System* that receives a *Reference (Desired) Position and Heading* from the operator and compares them to the *Actual Position and Heading* of the vessel (acquired by a DGPS and other position reference systems). A *Kalman Filter* is used to avoid response to wave frequent-motions, to provide multiple sensor data fusion, to estimate the environmental forces and to increase the system robustness. In some cases, a feed-forward of the wind load is also included in the control loop.

Lastly, the *Thrust Allocation Algorithm*, which is the focus of this paper, is responsible to distribute the total forces and moment required by the DP System among the available actuators, in such a way that the delivered power is minimal.

Further details on the DP System can be found in Serraris (2009), Van Dijk and Aalbers (2001) and Sorensen (2011).

1.2. Thrust allocation

As the vessels usually have more thrusters than degrees of freedom, guaranteeing operation safety and better station keeping capability, the allocation of forces and moments required by the DP System is a redundant problem with non-unique solution. To select the best one, thrust allocation algorithms are employed, distributing the forces among the available thrusters in an optimal way, defined by the algorithm designer.

A general survey of the state-of-art in such algorithms can be found in Johansen and Fossen (2013), who detailed several desired objectives, as to minimize the difference between required and allocated forces or to minimize the power demanded by the system, and several methods to achieve the optimal solution, including linear, quadratic and non-linear programming, depending on the formulation of the objective function.

Some works, as Wei et al. (2013) and Shi-Zhi et al. (2011a), use a quadratic relation between thrust and power, which allows simple optimization methods as Lagrange multipliers, for the constrained quadratic problem, and pseudo-inverses, for the unconstrained quadratic problem (i.e. does not consider thrust saturation), with good application in dynamic simulations. Despite this, the exact relation between the required power and delivered

* Corresponding author.
E-mail addresses: felipe.arditti@usp.br (F. Arditti), felipe_lopes@tpn.usp.br (F.L. Souza), thiago@usp.br (T.C. Martins), eduat@usp.br (E.A. Tannuri).

http://dx.doi.org/10.1016/j.oceaneng.2015.06.021
0029-8018/

thrust is a more complicated function, as shown by Van Daalen et al. (2011), demanding non-linear approaches.

Different objective functions allow the algorithm designer to include, in the optimization problem, more realistic models, as slack variables to deal with the saturation (Johansen and Fossen, 2013), thruster-rudder propellers (De Wit, 2009), and thrust force in polar coordinates (Johansen et al., 2004), enhancing the effectiveness of the algorithm.

To accomplish non-linear optimizations, several methods have been proposed, as stochastic optimization based algorithms, like the EABC - Enhanced Artificial Bee Colony (Ren et al., 2014), and Genetic Programming (Shi-Zhi et al., 2011b), which can achieve the global optimal solution escaping from local minimums, but involving high computational costs. De Wit (2009), however, used numerical algorithms, as Sequential Quadratic Programming (SQP), which searches for a local minimum in a deterministic way with known computational effort.

It is, also, interesting to mention some novel approaches to the allocation problem, as those developed by Veksler et al. (2012) and Rindarøy (2013). Those works deal directly with the power management system (PMS), avoiding load variations, counteracting external equipment, to achieve a more fuel economic behaviour than just power optimization. Those works also consider dynamic constraints, which deals with the finite change rate of the thrusters.

Another advanced solution concerns avoiding hydrodynamic interaction between the thrusters, usually treated with forbidden zones which cannot be occupied by the effectors (Johansen and Fossen, 2013), but the thruster–hull interaction usually is not considered in a consistent way in the most existing algorithms. A systematic method for considering hydrodynamic interaction in the allocation algorithm is the main contribution of this article.

Fig. 1 presents an example of an optimized thrust allocation. Both allocations respect the commanded force of 500 kN, but the second allocation optimizes the result, by avoiding interactions between thrusters, and saves approximately 40% power.

2. Hydrodynamic interaction effects and definition of the efficiency function

The hydrodynamic interaction effects on thrusters significantly affect the delivered thrust (Cozijn and Hallmann, 2013), therefore they should be considered during DP operations. Furthermore, the TRUST JIP is a Joint Industry Project with more than 20 companies, including thruster manufacturers, vessel operators, ship-yards and engineering companies, which aims at improving the understanding of thruster-interaction effects during DP operations.

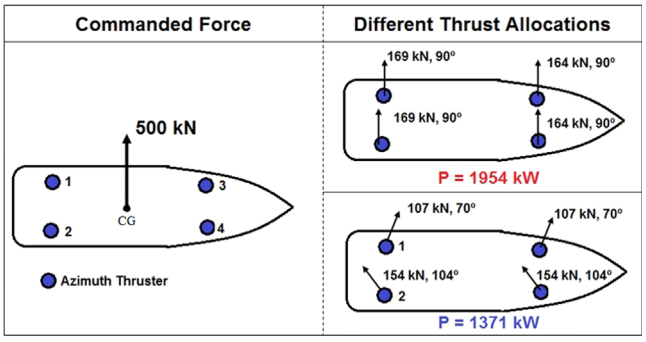

Fig. 1. Example of an optimized thrust allocation (Arditti and Tannuri, 2011).

2.1. Hydrodynamic interactions

First, the interaction effects addressed herein are thruster–hull and thruster–thruster. Initially they are explained and, then, the method developed to consider these effects in the thrust allocation algorithm is detailed.

2.1.1. Thruster–hull interaction

This effect is caused mainly by the drag and pressure forces on the hull, due to the wake flow of the thrusters. It also includes the Coanda effect (change in the form of the thruster water jet according to the form of the hull) and the deflection of the water jet. The thruster–hull interaction mainly depends on the form of the hull, in some cases on the pontoon of a platform (Fig. 2) and other underwater equipment, and on the thruster position. Recent studies demonstrate that the efficiency due to this interaction can drop by 40% (Cozijn and Hallmann, 2013). More details can be found in Ekstrom and Brown (2002).

2.1.2. Thruster–thruster interaction

The interaction between thrusters, usually azimuth thrusters, happens when they are close to each other. It is possible to observe the effects of drag and a decrease of efficiency when one thruster works in the wake stream of another. Only the effects of physical proximity between thruster structures are taken into account in this paper.

This interaction is typically avoided by defining forbidden zones for some azimuth angles, where severe interaction occurs. Fig. 3 presents an example of a forbidden zone definition in order to avoid interactions between the azimuth thruster centrally

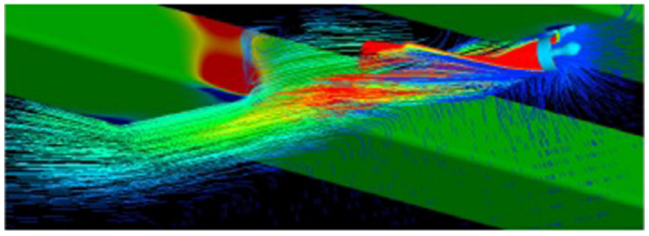

Fig. 2. Thruster–hull interaction (Jürgens et al. 2008).

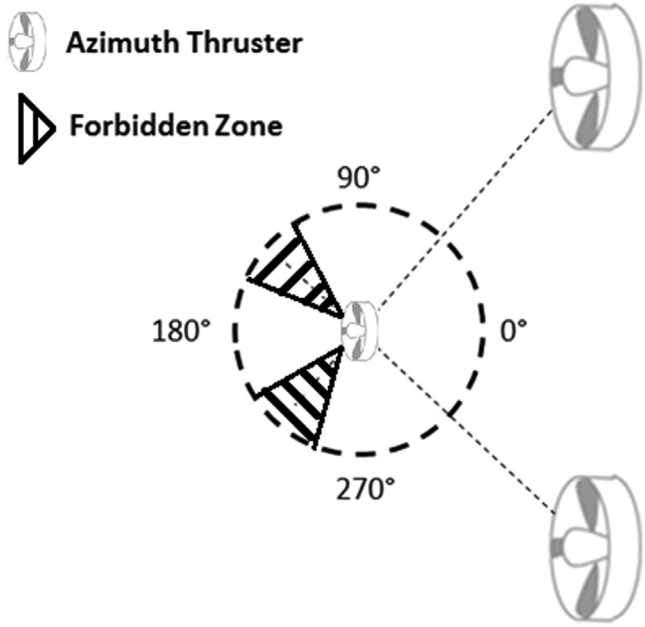

Fig. 3. Forbidden zones.

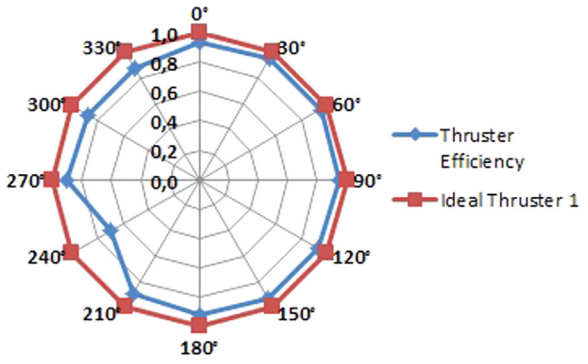

Fig. 4. Azimuth thruster representation considering its efficiency and ideal representation.

placed and two other thrusters closely positioned. Note that the azimuth angle refers to the direction of the force it generates (the wake stream flows in the opposite direction).

2.2. Efficiency function

In order to quantitatively represent the hydrodynamic interaction effects in the reduced generated thrust, an efficiency curve is suggested. The efficiency is defined as the ratio between the delivered thrust (T), considering the thruster in the vessel (with all the implied interactions, such as thruster–hull), and the thrust operating in open water (bollard pull - T_0), as represented in Eq. (1).

$$\eta = \frac{|T|}{T_0} \tag{1}$$

Note that the efficiency curve must be developed in polar coordinates in order to represent the azimuth thruster, since it can rotate 360°, and, for each azimuth angle, the efficiency reduction should change, due to the different directions of the jet stream. Fig. 4 presents an example of an efficiency curve.

2.3. Calculation of an efficiency curve

In order to verify the possibility of considering the efficiency functions in the thruster allocation algorithm, they were defined for two vessels and thrust allocation simulations were done considering them. The first case has efficiency data found in different bibliography, whereas the second case has efficiency data from experimental simulation.

2.3.1. Vessel 1 – theoretical efficiency curve

Fig. 5 presents the efficiency curves of the thrusters of Vessel 1. Since this vessel does not have a model, the efficiency drop due to thruster–thruster interaction was estimated according to the theory presented in Moberg and Hellstrõm (1983). The thruster–hull interaction decreases the efficiency by 20% when the water jet travels along the whole hull of the vessel, according to Ekstrom and Brown (2002).

2.3.2. Vessel 2 – experimental efficiency curve

A different approach to obtain the efficiency curves of the thrusters is through experiments with small scale vessel model, since it is not possible to analytically determine the efficiency curve due to the several interaction effects (Dang and Laheij, 2004). The experimental method used was to measure the thrust generated in different azimuth angles ($T(\alpha_i)$), and compare it with the bollard pull thrust (T_0). Note that this method only captures the effects of physical proximity between thrusters.

The design of Vessel 2 is shown in Fig. 6.

The thrust test conducted is shown in Fig. 7. The equipment used is:

1) A load cell with two independent Wheatstone bridges (Surge and Sway directions), to measure the tension generated by the forces that the thrusters produce. Note that the load cell is attached to the gravitational centre of the vessel.
2) A computer to command the thrusters and obtain the tension generated by the load cell through the AD converter.
3) A signal processing board to aquire the tension generated by the load cell.
4) An AD converter for communication between the signal processing board and the computer.
5) A wireless radio transmitter and receiver to command the thrusters (the commands come from the computer).
6) Some test masses for calibrating the load cell.

Initially, the load cell should be calibrated, which was performed using the test masses. The procedure for calibrating the load cell is to measure the voltage (V) generated by the load cell according to the test masses added to generate forces in Surge and Sway (F_x and F_y) directions, with independent measurements for each direction (V_x and V_y). Once these values are obtained, it is possible to linearly relate the tension generated by the load cell with the forces in each direction (Eq. 2).

$$K_x = \frac{F_x}{V_x}$$
$$K_y = \frac{F_y}{V_y} \tag{2}$$

After the calibration, the thrusters (one by one) are commanded to generate thrust in all azimuth angles (0°360°), at intervals of 30°, to determine their efficiency at different azimuth angles. At each simulated azimuth angle, V_x and V_y are obtained. Therefore, F_x and F_y are obtained through their relation with K_x and K_y.

With the forces produced by the thruster in the Surge (F_x) and Sway (F_y) directions, its module is calculated by:

$$T = \sqrt{F_x^2 + F_y^2} \tag{3}$$

The efficiency curves are shown in Fig. 8, and the form of them are related with the hydrodynamic interaction effects.

Comparing the results with the hypothesis for each interaction, it can be noticed that the method to determine the efficiency curves was qualitatively efficient. Therefore, the experimental method can represent different types of interference (between thrusters and thruster–hull). Furthermore, the polar coordinates representation for the efficiency curve is ideal to account for all the interaction phenomena.

3. Mathematical formulation of the optimization problem

After defining the method for dealing with the hydrodynamic interaction effects, the thrust allocation problem should be formulated. Note that it is an optimization problem, as explained in the introduction.

The functional to be minimized is the total power that is the summation of the individual power consumed by each thruster. Note, in Eq. (4), c_i is a constant value, which depends on the water density and on the diameter of the thruster, and T is the commanded thrust. Observe that the power consumed by a thruster is usually calculated by its torque multiplied by its rotation speed, and these values depend on the advance speed of the propeller. For DP situations, though, this value does not vary much, (Dang and Laheij, 2004), and the power consumption is fairly approximated to

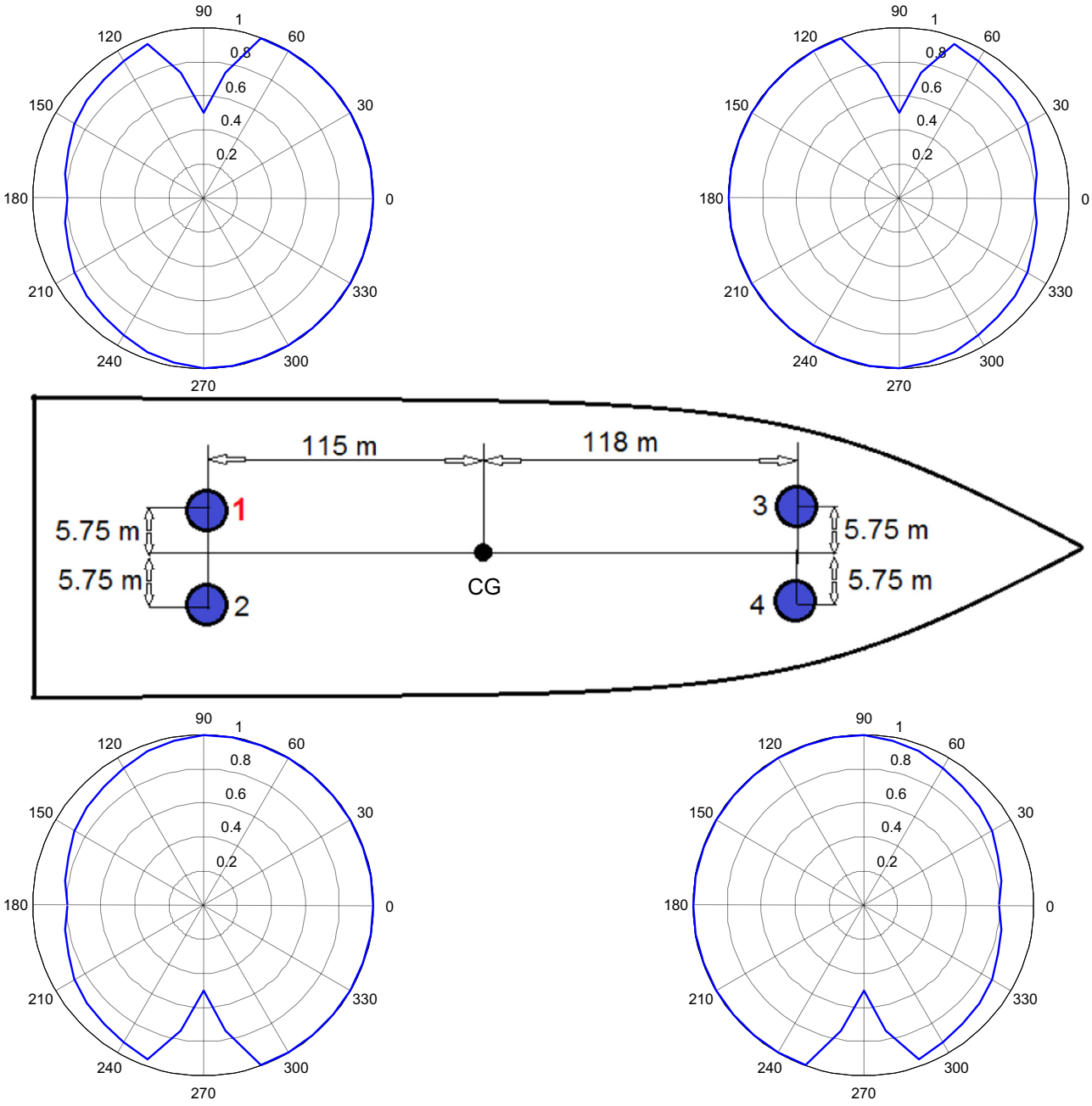

Fig. 5. Efficiency curves of the thrusters of Vessel 1.

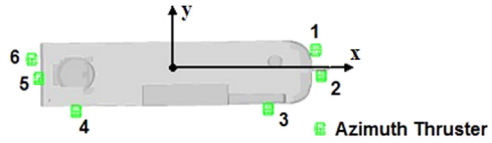

Fig. 6. Vessel 2.

the objective function shown in Eq. (4). Note that Jenssen and Realfsen (2006), Van Daalen et al. (2011), Dang and Laheij (2004) and Tannuri and Morishita (2006) considered the same approximation for power consumption.

In order to guarantee that the forces required by the Control System are matched by the total forces generated by the set of actuators (considering the interaction effects), a set of equalities is defined (R). Note that α is the azimuth angle in which the thruster is positioned and η its efficiency in the respective azimuth angle.

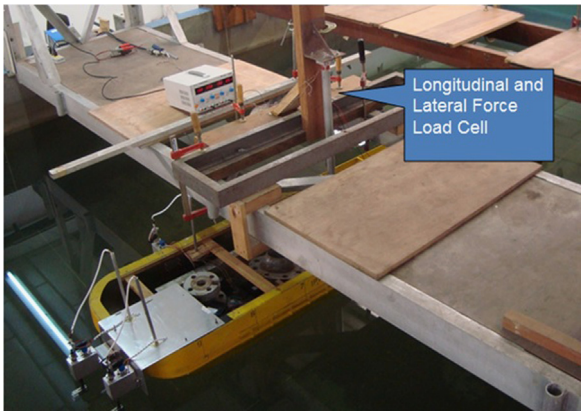

Fig. 7. Thrust test.

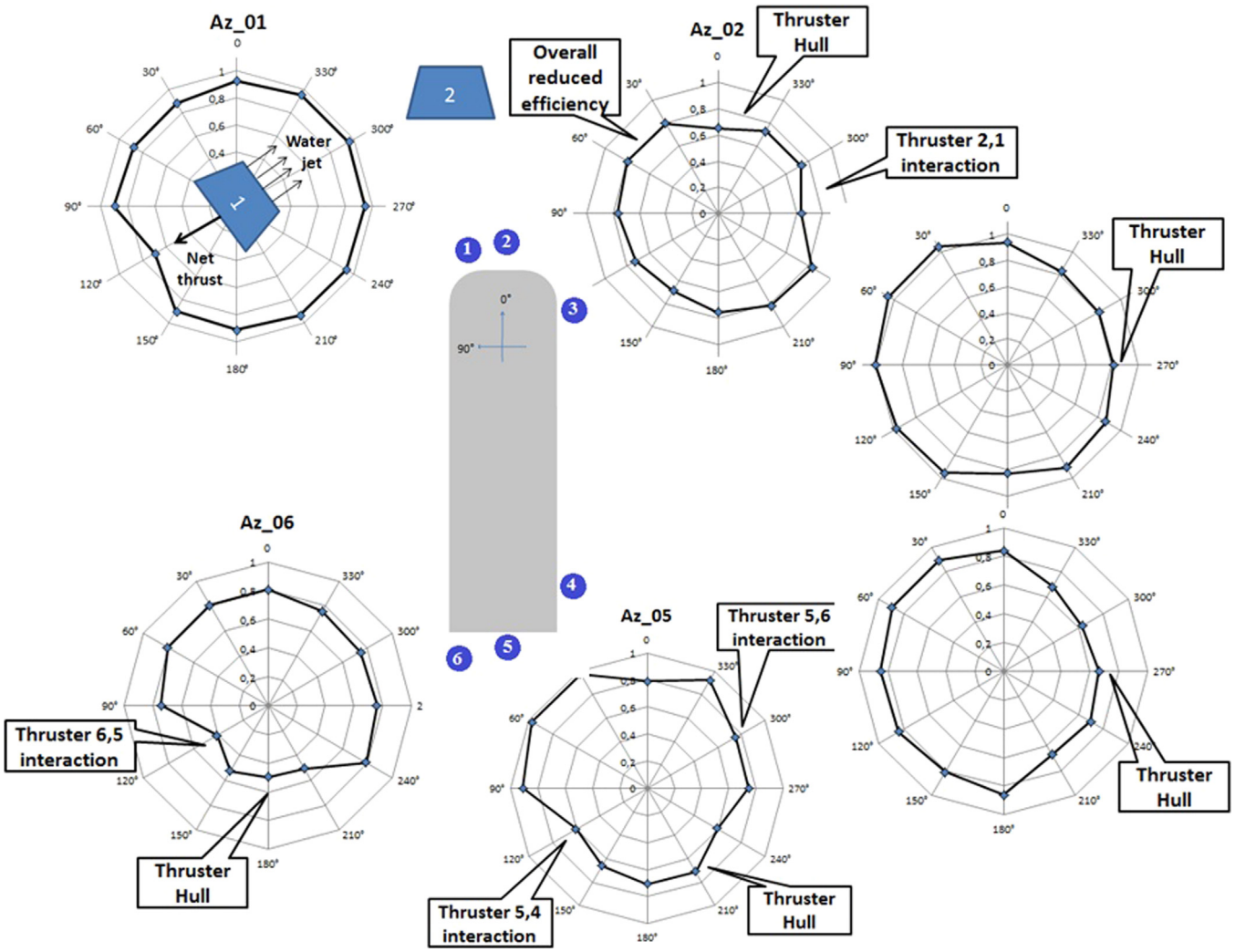

Fig. 8. Efficiency curves of Vessel 2 thrusters.

Finally, the saturation of the thrusters is addressed, since the thrusters cannot generate infinite thrust. Hence, a set of inequalities (I) represents the maximum thrust that can be generated by each thruster.

$$\underset{T,\alpha}{\text{Min}} \sum_{i=1}^{N} c_i(\rho, D) \cdot T_i^{\frac{3}{2}}$$

$$R\begin{cases} \sum_{i=1}^{N} T_i \cdot \cos\alpha_i \cdot \eta_i - F_x = 0 \\ \sum_{i=1}^{N} T_i \cdot \sin\alpha_i \cdot \eta_i - F_y = 0 \\ \sum_{i=1}^{N} [T_i \cdot \eta_i \cdot (x_i \cdot \sin\alpha_i - y_i \cdot \cos\alpha_i)] - M_z = 0 \end{cases} \quad (4)$$

$$I: \{T_i \le T_{max_i}$$

4. Thrust allocation algorithm

After defining the thrust allocation problem as an optimization problem with an objective function (power), equalities constraints (total force to be generated), and inequalities constraints (saturation), the developed thrust allocation algorithm is presented. The optimization problem is solved by a Sequential Quadratic Programming (SQP) method, whose concept and structure are detailed hereafter. Briefly, the SQP method (Nocedal and Wright, 2002) consists in:

1) Locally approximating a complex problem.
   a. The nonlinear equalities are approximated by a set of linear equations (R_L).
      i. $R_L: A \cdot [T, \alpha] = b$
   b. The objective function is approximated by a quadratic function.
      i. Quadratic $\Lambda = [T]a_1[T]^T + a_2[T]^T + a_3$
2) Solving the local Quadratic Programming (QP) problem:

$$\begin{aligned} &\text{Quadratic } \Lambda = [T]a_1[T]^T + a_2[T]^T + a_3 \\ &R_L: A \cdot [T, \alpha] = b \\ &I: \{T_i \le T_{max_i} \end{aligned} \quad (5)$$

3) And, from the new solution, repeating the steps above, using a convergence factor to stop the process.

QP refers to a class of optimization problems that has quadratic objective function and linear constraints, for which many solutions have already been developed. Therefore, approximating the thrust allocation problem by a quadratic optimization can be very interesting.

4.1. Thrust allocation algorithm structure

The developed algorithm structure is shown in Fig. 9.

4.1.1. Initial guess

The initial guess of the thrust allocation algorithm is calculated regardless of the hydrodynamic interaction phenomena and saturation. Furthermore, this step considers the power as a quadratic function. Finally, it is the solution of a simpler optimization problem solved by the Lagrange Multiplier Method (Nocedal and Wright, 2002), as represented below (note that it considers the force restrictions in Surge, Sway and Yaw).

The chosen initial guess is interesting because it is solved by easy computations and it is generally close to the final solution, which is very important for numerical optimization algorithms (Eq. 6).

$$L = \text{Quadratic}\,\Lambda - \sum_{i=1}^{3} \lambda_i \cdot h_i \tag{6}$$

4.1.2. Problem organization

The problem organization is the application of the SQP simplifications on the last solution. The force equations (R) are approximated by linear equations, as shown in Eq. (7), using Taylor Approximation, whilst the power equations are approximated by a quadratic equation, as presented in Eq. (8), also using Taylor approximation.

$$R_L = R(T_0,\alpha_0) + \sum_{i=1}^{N} \frac{dR(T_0,\alpha_0)}{dT_i}(T_i - T_{0_i}) + \sum_{i=1}^{N} \frac{dR(T_0,\alpha_0)}{d\alpha_i}(\alpha_i - \alpha_{0_i}) \tag{7}$$

$$\text{Quadratic}\,\Lambda = \sum_{i=1}^{N} c_i \cdot T_{0_i}^{\frac{3}{2}} + \sum_{i=1}^{N} \frac{\partial\left(c_i \cdot T_i^{\frac{3}{2}}\right)}{\partial T_i} \cdot (T_i - T_{0_i}) + \frac{1}{2} \cdot \sum_{i=1}^{N} \frac{\partial^2\left(c_i \cdot T_i^{\frac{3}{2}}\right)}{\partial {T_i}^2} \cdot (T_i - T_{0_i})^2 \tag{8}$$

4.1.3. Quadratic optimization (QP)

The quadratic optimization is the main part of the thrust allocation algorithm. Initially, it is checked (Simplex Check, detailed later) whether the problem can be solved considering the saturation of the thrusters and the required forces. If it is possible to solve the problem in these conditions, the Active-Set method performs the quadratic optimization; otherwise the Saturation Protocol starts (the Saturation Protocol is explained in Section 4.1.6), as represented in Fig. 10.

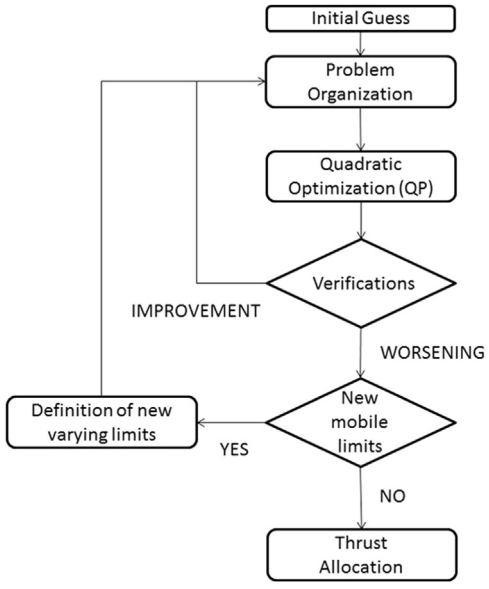

Fig. 9. Thrust allocation algorithm structure.

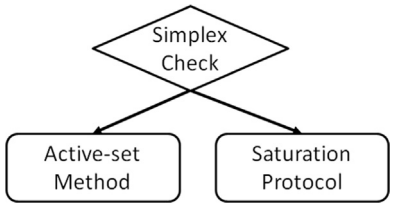

Fig. 10. Thrust allocation algorithm logic.

Table 1 presents the relation of the physical interpretation, the actual equations and how the equations are mathematically referred.

The Simplex, used to check allocation feasibility, is a well-known optimization algorithm for linear problems (Nocedal and Wright, 2002). Note this is a linear problem because the set of equalities was linearized (R_L) and the set of inequalities (I) is already linear. A linear objective function is also defined for the Simplex, as presented in Eq. (9).

$$\underset{T,\alpha}{\text{Min}} \sum_{i=1}^{N} c_i(\rho, D) \cdot T_i$$

$$R_L : \begin{cases} R_1(T_0,\alpha_0) + \sum_{i=1}^{N} \frac{dR_1(T_0,\alpha_0)}{dT_i}(T_i - T_{0_i}) + \sum_{i=1}^{N} \frac{dR_1(T_0,\alpha_0)}{d\alpha_i}(\alpha_i - \alpha_{0_i}) = 0 \\ \text{Analog for Sway } (R_2) \text{ and Yaw } (R_3) \end{cases}$$

$$I : \{T_i \le T_{max_i}$$

(9)

Briefly, the Simplex optimization will try to solve the problem activating and deactivating all the possible combinations of the inequalities. For every solution it finds, it tests whether this solution is the global optimum based on the Karush–Kuhn–Tucker (KKT) conditions (Nocedal and Wright, 2002).

Once observed that the optimization problem represented in Eq. (9) can be solved (there is a solution from the Simplex optimization), the Active-Set Method is applied to perform the quadratic optimization.

This iterative method verifies which inequalities should be active in the solution. The basic strategy behind this method is considering the objective function and only a set of inequalities active at each step (similar strategy to the Simplex algorithm). After solving this sub problem, it is verified which inequalities are disrespected (and should therefore be active in the next iteration), and which inequalities do not represent an obstacle to the pursuit of the minimum (and should therefore not be considered in the next iteration).

Fig. 11 presents a simple quadratic optimization problem that is solved with the active-set method, for further detailing the procedure. Note that W is an integer vector that contains the active inequalities for each interaction.

1. In the initial state restriction, 2 (R_2) is active.

Table 1
Required forces and inequalities.

Physically	Equations	Mathematically
Required forces equations	R_L	Equalities
Saturation varying limits	I	Inequalities

2. The first step considers that R_2 should be respected; therefore, $W_2 = 1$. At the end of this step, it is verified that $\lambda_2 < 0$, hence should not be considered in the following step.
3. No inequalities are considered in this sub problem. The result is the global minimum, but it does not respect R_4.
4. R_4 must be respected; therefore, X_3 is in the segment that connects X_1 to X_2 respecting R_4.
5. R_4 is active; therefore, $W_4 = 1$. At the end of this iteration, it is verified that $\lambda_4 > 0$. Note that all $\lambda \geq 0$; hence, according to the KKT conditions (Nocedal and Wright, 2002), this is the best solution to the problem.

4.1.4. Verifications

After solving the quadratic optimization problem, two verifications are conducted in order to determine if the new solution is better than the previous one.

1) The first verification checks whether the forces are generated more precisely and the power has decreased, altogether.
2) The second one verifies whether the value of the Lagrangean (shown in Eq. 10) of the original problem (without simplifications) has decreased.

$$L = \sum_{i=1}^{N} c_i \cdot T_i^{\frac{3}{2}} - \sum_{i=1}^{3} \lambda_i \cdot R_i \tag{10}$$

If, at least, one verification is true, the new solution is better than the previous one and it is used as the initial step of the following iteration of the SQP method (with the same conditions).

If the two verifications are false, the new solution is worse than the previous one. Hence, the last solution is kept and the problem is solved considering a smaller simplification interval (the varying limits).

$$\delta_i = \alpha \cdot \delta_{i-1}$$
$$\alpha < 1 \tag{11}$$

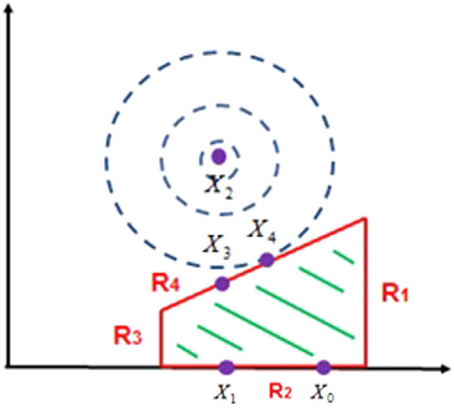

Fig. 11. Active-set method.

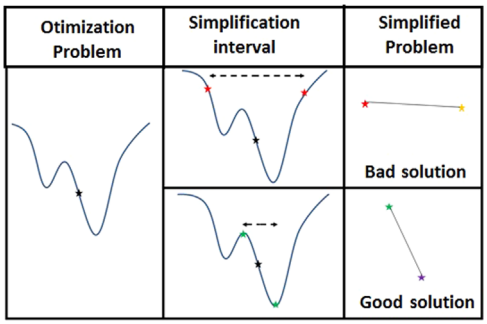

Fig. 12. Varying limits implementation.

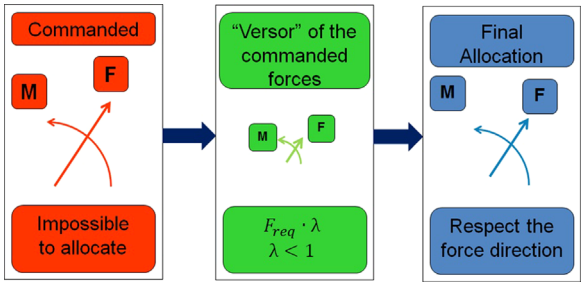

Fig. 13. Force generation in the direction of the Versor of the required force in the Saturation Protocol.

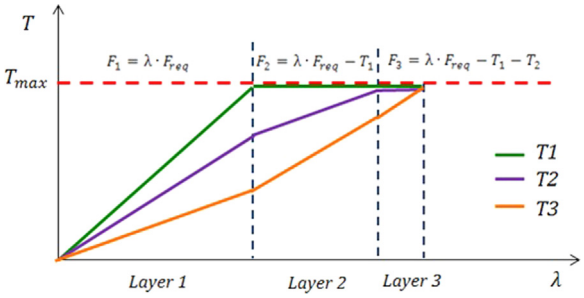

Fig. 14. Implementation of the Saturation Protocol.

4.1.5. Varying limits

The use of varying limits is not usual in the SQP method. However, it is an interesting solution because the Hessian of the objective function (Eq. 3) presents positive and null eigenvalues. The null eigenvalues refer to the contribution of the azimuth angles in the power consumption, which are of course null. Therefore, if the varying limits were not used, the QP algorithm would vary the azimuth angles infinitely to match the linearized equalities, which would not solve the allocation problem. Furthermore, the varying limits can be used to define the range for the simplifications performed by the SQP method.

The implementation of the varying limits in the SQP method is carried out according to the following procedure (shown in Fig. 12): an interval of simplification is initially defined; if it is too large, it leads to bad approximations and solutions (according to the verifications block). If that is the case, the range of approximations is diminished (varying limits) and a better solution can be found. This procedure is repeated until the varying limits are significantly small.

Note the implementation of the saturation is straightforward if the concept of varying limits is applied. The varying limits should respect these physical boundaries; therefore, if they cross them, they are set to those boundaries.

4.1.6. Saturation Protocol

The Saturation Protocol is the procedure followed by the thrust allocation algorithm when it is not possible to generate the required forces considering the saturation of the thrusters (T_{max}), verification performed by the Simplex check. Therefore, if it is not possible to generate the required forces, a compromise allocation should be selected. The strategy chosen is to generate the maximum force in the direction of the Versor of the required force, as shown in Fig. 13.

In order to generate the maximum force in the direction of the Versor of the required forces, the thrust allocation algorithm is used in a modified reallocation strategy, as presented in Fig. 14 (only 3 thrusters are represented for simplicity). At every layer of the reallocation, a binary search is performed in order to find the largest λ until one of the thrusters saturates. When one of the thrusters saturates, its thrust and azimuth angle are saved and a new layer to find a larger λ begins (as shown in Eq. 12).

Note the force generated by all the thrusters will always respect the direction of the required force, because the force produced by the saturated thrusters is considered a constant value in the following allocations.

$$\underset{T,\alpha}{\text{Min}} \sum_{i=2}^{N} c_i(\rho, D) \cdot T_i^2$$

$$R\begin{cases} \sum_{i=2}^{N} T_i \cdot \cos\alpha_i \cdot \eta_i + T_1 \cdot \cos\alpha_1 \cdot \eta_1 - \lambda \cdot F_x = 0 \\ \sum_{i=2}^{N} T_i \cdot \sin\alpha_i \cdot \eta_i + T_1 \cdot \sin\alpha_1 \cdot \eta_1 - \lambda \cdot F_y = 0 \\ \sum_{i=2}^{N} [T_i \cdot \eta_i \cdot (x_i \cdot \sin\alpha_i - y_i \cdot \cos\alpha_i)] + [T_1 \cdot \eta_1 \cdot (x_1 \cdot \sin\alpha_1 - y_1 \cdot \cos\alpha_1)] - \lambda \cdot M_z = 0 \end{cases}$$

$$I : \begin{cases} T_i \le T_{max_i} \\ T_1 = T_{max_1} \end{cases} \tag{12}$$

By using the modified reallocation strategy, it is possible to use an algorithm that has a power optimization objective in order to reach a different objective (generate the maximum force in the direction of the original required forces). The strengths and weaknesses of this strategy are presented in Table 2.

5. Numerical implementation and results

Numerical simulations were run to verify the efficiency of the developed thrust allocation algorithm and to compare it against Forbidden Zone (FZ) algorithms. These simulations were run for both of the vessels presented herein.

The FZ algorithm does not allow the azimuth angles to be defined in such angles in which the wake stream will hit another thruster, which means a 20° forbidden zone around the direction that connects two closely positioned thrusters. This algorithm is normally applied in DP Systems. Furthermore, an internal recursive algorithm assures that the total force allocated by this algorithm is equal to the commanded forces. This recursive algorithm emulates a closed loop controller, and considers the efficiency curves. This procedure is necessary because the FZ algorithm only accounts for the thruster–thruster interaction, disregarding the other sources of thruster efficiency reduction.

5.1. Vessel 1 simulations

The simulations performed with vessel 1 account for real environmental conditions. The procedure to simulate them is detailed in Arditti and Tannuri (2011). Furthermore, capability plots are used for the simulations.

Fig. 15 presents the power capability plot of the proposed allocation algorithm for vessel 1 in real environmental conditions. Note that the blue line represents the percentage of power consumed (compared with the total power of the vessel). Further simulations showed that the developed thrust allocation algorithm saves an average of 2% of power in relation to the FZ algorithm.

Fig. 16 presents a current capability plot for the proposed and FZ algorithms. The vessel is aligned with the wind and the waves, and the current rotates around the vessel. The blue and red lines are the maximum current speed for which the vessel could match the total environment forces.

Table 3 presents the main results from the current capability simulation. Note that the developed thrust allocation algorithm could handle a 5% higher mean current than the FZ algorithm, thus enlarging the operational window of the vessel.

5.2. Vessel 2 simulations

Several numerical simulations were run for the model of vessel 2. A different simulation technique was considered. Instead of using the capability plot, the simulations represent cases that could be experimentally verified. Note that, for these cases, the thrusters are commanded to produce a certain total force.

In all the simulated cases, the developed algorithm and the FZ algorithm reached the required forces. Furthermore, the developed algorithm was always more economic than the FZ algorithm regarding power consumption.

Fig. 17 exemplifies the results. In this case, the vessel should have produced the following required force: $[F_x = -7\ \text{N} \quad F_y = 7\ \text{N} M_z = 0]$. The developed algorithm was "clever" enough to reduce the utilization of T2, due to its lower efficiency (see Fig. 8). Also, it reduced the utilization of T5 and T6, that are not efficient in those directions according to the experiments due to significant thruster–hull interaction.

6. Experimental validation

The numerical simulations showed that the developed thrust allocation algorithm was more efficient than the FZ algorithm. Therefore, experimental analysis with Vessel 2 was also done to verify this statement.

The simulated algorithms were the developed thrust allocation algorithm, the FZ algorithm and the Simple Lagrangean Allocation (SLA).

The SLA is solved by a pseudo-inverse matrix definition that does not consider any of the hydrodynamic interaction effects. The SLA allocation is simply based on a Lagrange Multiplier optimization method. This algorithm is normally used for basic simulations of the vessel in early design stages. The objective of simulating this algorithm is to verify the importance of the interference effects and check whether it is possible to match the commanded forces neither explicitly considering the hydrodynamic interaction effects nor emulating them.

Table 2
Strengths and weaknesses of the Saturation Protocol.

Strengths	Weaknesses
Robustness: saturate almost all the thrusters (uses the reserves). **Best step solution**: solves the problem according to the developed thrust allocation optimization method on every layer. **Direction prioritization**: it is possible to change the Versor in order to prioritize a specific force or moment. This implementation was not studied.	**Different objectives**: does not guarantee the best mathematical solution for error minimization because a power optimization algorithm is used.

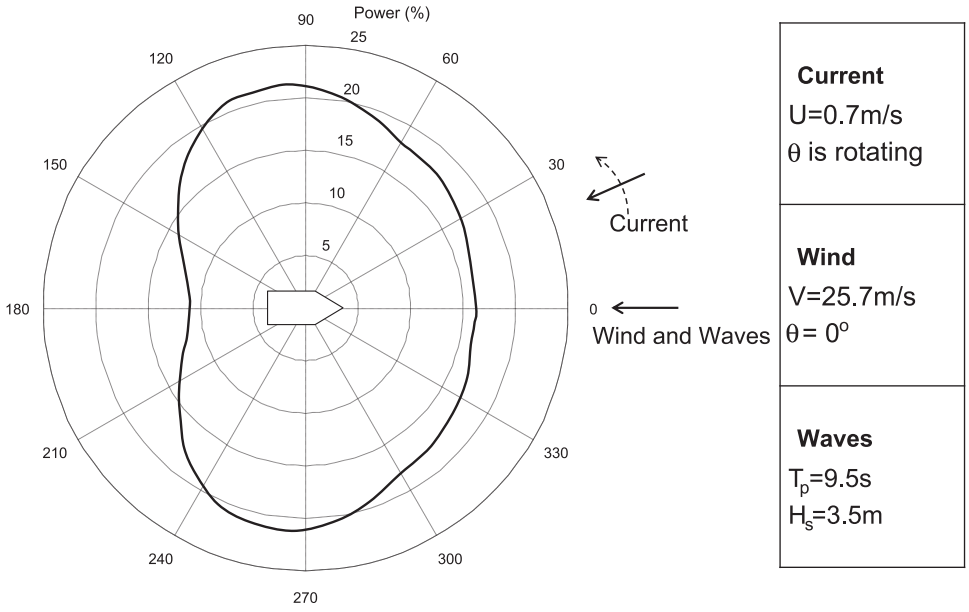

Fig. 15. Power capability plot of Vessel for real environment conditions.

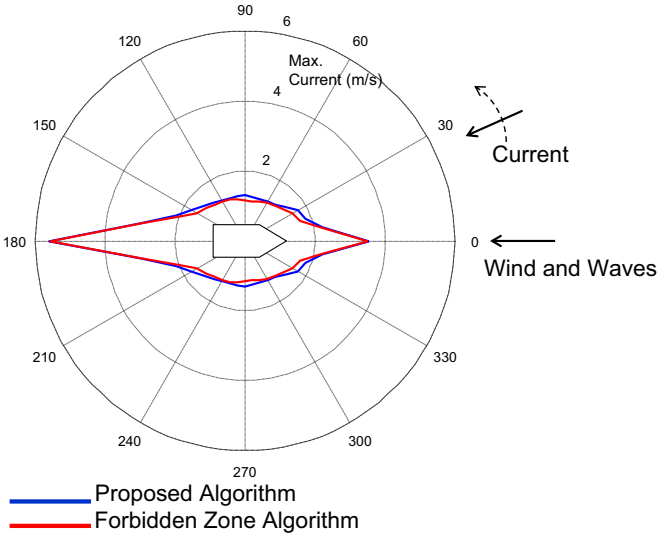

Environmental Conditions		
Current	**Wind**	**Waves**
U=maximum speed θ is rotating	V=25.7m/s θ = 0°	T_p=9.5s H_s=3.5m

Fig. 16. Maximum current capability plot of Vessel for real environment conditions.

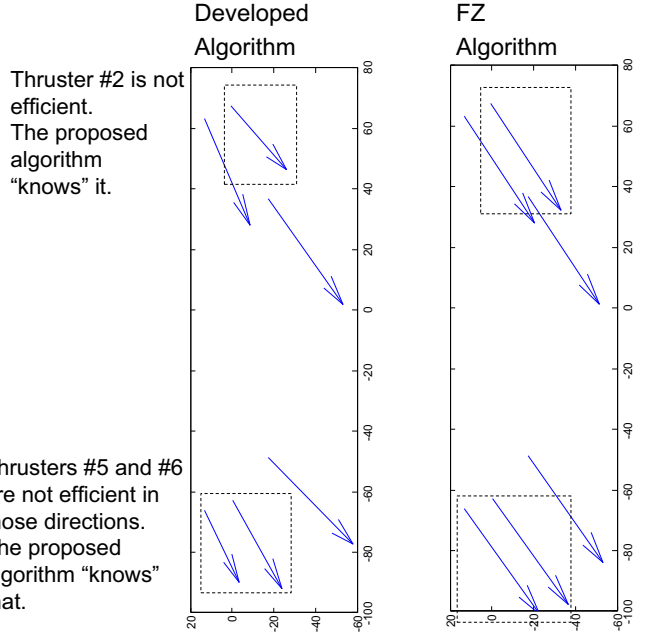

Fig. 17. Numerical comparison between the allocation algorithms for a required force of $\left[F_x = -7\ \mathrm{N} \quad F_y = 7\ \mathrm{N} \quad M_z = 0\right]$.

Table 3
Further information on the maximum current capability plot.

	Max (m/s)	Min (m/s)	Mean (m/s)
Proposed	5.61	1.26	1.84
FZ algorithm	5.59	1.15	1.75

6.1. Evaluation criteria

In order to analyse the results of the experimental simulations two criteria will be verified:

1) Difference between required forces and delivered forces (error).
2) Power consumption.

Note that the first criterion is more important than the second. Therefore, if any of the algorithms does not respect the first criterion (that guarantees the station keeping of the vessel), the second criterion will not be accounted for.

6.2. Simulation arrangement

The simulation arrangement has the same set-up and equipment as the one used to obtain the efficiency curves of the thrusters of Vessel 2 (presented in Fig. 7), referred as thrust test. Note that all the calibration steps previously described were repeated before the thrusters were turned on, in order to accurately measure the generated force. The simulations were carried out following this procedure:

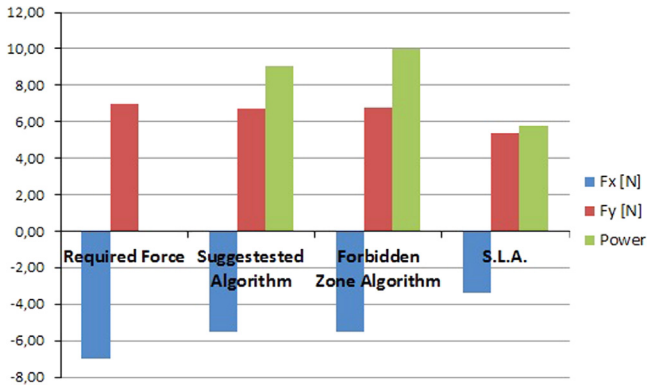

Fig. 18. Experimental comparison between three thrust allocation algorithms for a required force of $\left[F_x = -7\ \mathrm{N} \quad F_y = 7\ N \quad M_z = 0\right]$.

Table 4
Summary of the force generation experiments, forces in Newton and normalized power.

	Exp. 2			Exp. 3			Exp. 4			Exp. 5		
	F_x [N]	F_y[N]	Power	F_x[N]	F_y[N]	Power	F_x[N]	F_y[N]	Power	F_x[N]	F_y[N]	Power
Comm.	0	−10		7	−7		−7	−7		7	−7	
Prop.	−0.4	−8.8	10.0	8.1	−6.9	10.0	−5.5	−6.4	10.0	8.1	−6.9	10.0
Forb. Z.	−0.4	−8.9	10.4	8.1	−7.3	10.5	−5.8	−5.6	10.8	8.1	−7.3	10.5
S.L.A.	0.2	−5.9	6.4	6.5	−5.3	6.8	−3.9	−4.3	6.7	6.5	−5.3	6.8

1) A total required force was defined.
2) The three thrust allocation algorithms solved the problem.
3) The result of each thrust allocation (one by one) was commanded to the vessel through the radio transmitter and the thrusters were turned on.
4) Finally, with all thrusters working, the force was measured by the load cell. Remember that the experimental arrangement allows us to measure F_x and F_y generated by the thrusters of the model.
5) Finally the measured forces were compared with the required force (F_{req_x} and F_{req_y}).

6.3. Main results

The first experiment (with the same required forces as the one shown in Fig. 17) is shown in Fig. 18. It exemplifies the proximity between the delivered and the required forces for the thrust allocations performed with the proposed and the FZ algorithms (the developed thrust allocation algorithm saved about 10% power in relation to the FZ algorithm). Moreover, the forces delivered by the SLA algorithm were significantly smaller than the required ones.

Table 4, has a summary of all the experiments. Note the proximity between the commanded force, the force generated by the suggested algorithm and by the FZ Algorithm. The proposed algorithm saved 5% power (on average) compared with the FZ algorithm.

Finally, the experimental results were very similar to the numerical ones. In every case, the proposed thrust allocation algorithm and the FZ algorithm fairly generated the required forces. Furthermore, the proposed allocation method saved more power than the FZ algorithm. On the other hand, the SLA algorithm did not match the required forces, hence demonstrating that it is not possible to match the required forces without considering the hydrodynamic interaction effects.

7. Conclusions

The results demonstrate the need to consider the hydrodynamic interaction effects within the thrust allocation.

These interactions were represented by means of efficiency curves, a robust and general method to represent any kind of interaction. Moreover, the experimental building of the efficiency curves presented results in accordance with the expected hydrodynamic phenomena, thus validating the method.

The numerical simulations with vessel 1 indicate power economy and enlargement of the operational window.

The numerical and experimental simulations of vessel 2, again, presented power advantages when considering the interaction effects within the thrust allocation. Furthermore, the experimental results demonstrate that the force generation is significantly more accurate when the hydrodynamic interaction data is provided. This can be explained considering that including experimental data approximates the mathematical problem to reality. Moreover, the operation safety increases when the force generation precision increases.

Regarding the algorithm, the SQP strategy combined with the Active-set method to solve the intermediate QP problem, has proven robust, efficient, and, most importantly, able to deal with the nonlinearity of the complex optimization problem.

Acknowledgements

Some of the tests presented herein were performed as part of the TRUST JIP. The authors would like to express their gratitude to the TRUST participants for their permission to use the JIP data to prepare this paper.

The authors also acknowledge Petrobras for the technical and financial support to this research, the Brazilian Research Council (CNPq Proc. 377946/2013-3, 308645/2013-8 and 306415/2012-7) and São Paulo Research Foundation (FAPESP Proc. 2010/11903-3) for the research grants.

References

Arditti, F., Tannuri, E.A., 2011. Thrust Allocation Algorithm for DP Systems Considering the Interference between Thrusters and Thruster–Hull 2011. COBEM, Natal, Brazil.

Cozijn H., Hallmann R., 2013. Thruster-interaction effects on a DP semi-submersible and a drill ship - measurements and analysis of the thruster wake flow. In: Proceedings of the OMAE2013-11138, OMAE Conference. Nantes.

Dang J., Laheij H., 2004. Hydrodynamic aspects of steerable thrusters. In: Proceedings of the Dynamic Positioning Conference, Marine Technology Society.

De Wit, C., 2009. Optimal Thrust Allocation Methods for Dynamic Positioning of Ships Master thesis. Delft University of Technology, Holland.

Ekstrom L., Brown D.T., 2002. Interactions between thrusters attached to a vessel hull. In: Proceedings of 21st International Conference on Offshore Mechanics and Artic Engineering. OMAE 02, Oslo, Norway.

Jenssen N.A., Realfsen B., 2006. Power optimal thruster allocation. In: Proceedings of the Dynamic Positioning Conference. Marine Technology Society. Houston.

Johansen, T.A., Fossen, T.I., Berge, S.P., 2004. Constrained nonlinear control allocation with singularity avoidance using sequential quadratic programming. IEEE Trans. Control Syst. Technol. 12 (1), 211–216.

Johansen, T.A., Fossen, T.I., 2013. Control allocation - a survey. Automatica 49 (5), 1087–1103.

Jürgens D., Palm M., Amelang A., Moltrecht T., 2008. Design of reliable steerable thrusters by enhanced numerical methods and full scale optimization of thruster–hull interaction using CFD. In: Proceedings of the MTS DP Conference. Houston.

Moberg S., Hellstrõm S.A., 1983. Dynamic Positioning of a four column semi-submersible. Model testes of interaction forces and a philosophy about optimum strategy when operating thrusters. In: Proceedings of Second International Symposium on Ocean Engineering and Ship Handling. pp 443–480.

Nocedal, J., Wright, S.J., 2002. Numerical Optimization Chapters 3, 13, 16 and 18. Springer, Berlin, Second edition.

Ren F., Wu D., Yang G., Yin, Z., 2014. An intelligent thrust allocation method for dynamic positioning based on enhanced artificial bee colony algorithm. In: Proceedings of the IEEE 9th Industrial Electronics and Applications. ICIEA, pp. 972–977.

Rindarøy, M., 2013. Fuel Optimal Thrust Allocation in Dynamic Positioning Master degree thesis. Institutt for Teknisk Kybernetikk, Norway.

Serraris J.J., 2009. Time-domain analysis for DP simulations. In: Proceedings of the OMAE2009-79587, OMAE Conference. Honolulu.

Sorensen, A.J., 2011. A survey of dynamic positioning control systems. Annu. Rev. Control 35 (1), 123–136.

Tannuri, E.A., Morishita, H.M., 2006. Experimental and numerical evaluation of a typical dynamic positioning system. Appl. Ocean Res. 28, 133–146.

Van Daalen E.F.G., Cozijn J.L., Loussouarn C., Hemker P.W., 2011. A generic optimization algorithm for the allocation of DP actuators. In: Proceedings of the OMAE2011-49116, OMAE Conference. Rotterdam.

Van Dijk R.R.T., Aalbers A.B., 2001. What happens in water - the use of hydrodynamics to improve DP. In: Proceedings of the MTS Dynamic Positioning Conference. Houston.

Veksler A., Johansen T.A., Skjetne R., 2012. Thrust allocation with power management functionality on dynamically positioned vessels. In: Proceedings of the American Control Conference.

Shi-Zhi, Y., Wang, L., Sun, P., 2011a. Optimal thrust allocation logic design of dynamic positioning with pseudo-inverse method. J. Shanghai Jiaotong Univ. (Sci.) 16 (1), 118–123.

Shi-Zhi, Y., Wang, L., Zhang, S., 2011b. Optimal thrust allocation based on fuel-efficiency for dynamic positioning system. J. Ship Mech. 15 (3), 217–226.

Wei, Y., Fu, M., Ning, J., Sun, X., 2013. Quadratic programming thrust allocation and management for dynamic positioning ships. TELKOMNIKA Indones. J. Electr. Eng. 11 (3), 1632–1638.